CSC2431: Final Report draft

Rohan Chandra 996274142

Abstract:

While various methods of CAD of lung nodule detection in CT scans have been proposed, a recurring paradigm in existing methods is the focus on identifying nodules based on shape and intensity characteristics. Particularly, many methods have focused on distinguishing the more spherical shape of lung nodules from the more elongated and cylindrical anatomical features of the lung, such as is the case of blood vessels. The proposed method seeks to exploit curvature information obtained from eigenanalysis of the image Hessian to create a better weighting mechanism for HoG methods, allowing the histogram to be influenced more heavily by voxels that belong to more blob like structures as oppose to elongated or planar structures. The weighted histogram would then be used to create a 3D shape descriptor for a volume of interest that can then be classified by a linear SVM.

Related works:

Common methods for lung nodule detection involve template matching based on gradient intensities and orientation [1,2,3], identifying nodules based on the properties of an ellipsoid fit to the region of interest [4] or of properties of a volume of interest's eccentricity and circularity [5]. In these cases, the methods attempt to exploit underlying shape properties common to lung nodules for the purpose of detection. Particularly, shape information is used to distinguish the more spherical shaped cancer lesions from the more elongated shaped blood vessels. Sato, Yoshinobu, et al [6] showed that local shape analysis obtained from eigen analysis of the image Hessian could be used to distinguish different types of tissue when rendering visualizations of scanned data. Mendonça, Paulo RS, et al. [7] developed a model-based analysis of local shape for lesion detect in CT scans, but used curvature tensor analysis rather than analysis of the image Hessian, to avoid shape mischaracterizations that can occur at inflection points of an intensity profile. Some of these issues arise in methods that use averaged characteristics of the hessian to form feature sets [8]. Similarly, Epstein et al [9] methods for detecting colonic polyps based on local curvature features, as well as Daniels, Florie, et al [10] showed that eigenanalysis of the image Hessian can be used to distinguish tube, blob and plane like structures within an organ, particularly when distinguishing between nodules and blood vessels or organ walls. Thus, the propose method seeks to adapt the general structure outlined in Yang, Periaswamy, and Wu [1], but create a shape descriptor that is more heavily influenced by voxel that belong to lung nodules as oppose to voxels that originate from irrelevant anatomic structure such as blood vessels.

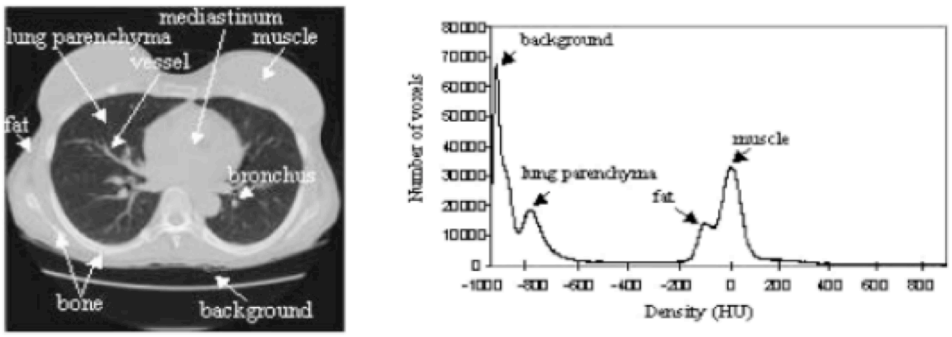

Figure 1: A) Chest CT slice, with anatomic structure of the lung indicated, B) Corresponding volumetric density histogram annotated with typical lung anatomic structure (image adopted from ZHAO et al, [3])

Lung Volume Segmentation:

The algorithm automatically generates a 3d volumetric mask to isolate the internal volume of the lungs from each CT scan, to avoid analysis of irrelevant portions of the entire CT scan. The process used in this method is similar to the methods for lung volume extraction in CT scans presented in [1, 2, 3, 11], and focuses on identifying voxels within the CT scan whose associated density falls within a predetermined range. Analysis conducted in [3, 11] showed that the majority of relevant lung tissue could be isolated by thresholding the source image between -900 and -370 Hounsfield units (see figure 1: A), as the majority of bone, fat and muscle structure is associated with a distinguishable density value outside of this range. However, voxels within the background may fall within the target threshold range (see figure 1: B). To remove these sections, the thresholded mask is divided into components, via a 3D connected components method based on the union find algorithm. Any connected component that consists of too few voxels are discarded, as well as any component that touch the image boundary, leading to the mask seen in figure 2: C. Finally, to fill in the small gaps present in the mask and to remove elongated thin components, the mask is processed using a 3D morphological closing operator to produce the final 3D lung volume as seen in figure 2: D.

Figure 2: (from left to right):
A) A slice of the original ct scan, B)The initial thresholded mask, C) the mask after all connected components that touch the image boundary are removed, D) The final lung volume mask after 3d image closure

Image derivatives:

In the presented method, the first and second order image intensity derivatives are computed using 3D Deriche filters [12] as separable 1D convolutions with normalization coefficients chosen according to the specifications presented in [13]. In this formulation, the following functions are defined:

Smoothing operator:

$$f_0(x) = c_0(1 + \alpha|x|)e^{-\alpha|x|}$$

First Derivative operator:

$$f_1 = c_1 x\alpha^2 e^{-\alpha|x|}$$

Second Derivative operator:

$$f_2 = c_2(1 - c_3\alpha|x|)e^{-\alpha|x|}$$

By construction, each function is proportional to the derivative of the previous function, except at x = 0, where the functions are not differentiable. These functions are used as convolution filters, which smooth the input image (the degree to which is controlled by the filter width) and generate the first and second order partial derivatives. The normalization coefficients c_0, c_1, c_2, c_3 are chosen such that

$$\int f_0(x)dx = 1$$

$$\int x f_0(x)dx = 1$$

$$\int f_2(x)dx = 0 \ \ and \ \ \int \frac{x^2}{2} f_2(x)dx = 1$$

To ensure that a convolution by these filters yield the correct derivatives when applied to polynomials. Then, the normalization coefficients are specified for discrete convolution as:

$$c_0 = \frac{(1 - e^{\alpha})^2}{1 + 2e^{-\alpha}\alpha - e^{-2\alpha}}$$

$$c_1 = \frac{-(1 - e^{-\alpha})^3}{2\alpha^2 e^{-\alpha}(1 + e^{-\alpha})}$$

$$c_2 = \frac{-2(1 - e^{\alpha})^4}{1 + 2e^{-3\alpha}\alpha - e^{-4\alpha}}$$

$$c_3 = \frac{(1 - e^{-2\alpha})}{2e^{-\alpha}}$$

Where the value of α controls the degree of smoothing. In practice α is chosen as 1 for the smoothing function and first order partial derivatives, and as 0.7 for second-order derivatives (where a larger degree of smoothing is required to avoid influence from noise). Then, to compute smoothed partial derivatives, the image, I(x,y,z) is convolved with the appropriate series of filters, for example the partial derivatives in x can be computed with the following convolutions:

$$\frac{dI}{dx} = (f_1(x)f_0(y)f_0(z)) * I$$

$$\frac{dI^2}{dx^2} = (f_2(x)f_0(y)f_0(z)) * I$$

$$\frac{dI^2}{dxdy} = (f_1(x)f_1(y)f_0(z)) * I$$

$$\frac{dI^2}{dxdz} = (f_1(x)f_0(y)f_1(z)) * I$$

Curvature:

Using the first and second order partial derivatives calculated in the previously described manner, a local curvature features can be computed. Using the second order Hessian matrix as the local shape descriptor:

$$H = \begin{bmatrix} \frac{dI^2}{dx^2} & \frac{dI^2}{dxdy} & \frac{dI^2}{dxdz} \\ \frac{dI^2}{dydx} & \frac{dI^2}{dy^2} & \frac{dI^2}{dydz} \\ \frac{dI^2}{dzdx} & \frac{dI^2}{dzdy} & \frac{dI^2}{dz^2} \end{bmatrix}$$

The principal curvature and principal directions can be computed as the eigenvalues and eigenvectors of the second order hessian matrix. The eigenvalues, λ_0, λ_1, λ_2, where $|\lambda_0| \leq |\lambda_1| \leq |\lambda_2|$, correspond to the rate of change in intensity along the intensity surface in the principal directions and can be used together to determine the local shape.

Eigenvalues	**Structure**
$\lambda_0 \cong 0, \lambda_1 \cong 0, \lambda_2 \cong 0$	Noise
$\lambda_0 \cong 0, \lambda_1 \cong 0, \lambda_2 < -H$	Bright plane
$\lambda_0 \cong 0, \lambda_1 \cong 0, \lambda_2 > H$	Dark plane
$\lambda_0 \cong 0, \lambda_1 < -H, \lambda_2 < -H$	Bright tube
$\lambda_0 \cong 0, \lambda_1 > H, \lambda_2 > H$	Dark tube
$\lambda_0 < -H, \lambda_1 < -H, \lambda_2 < -H$	Bright blob
$\lambda_0 > H, \lambda_1 > H, \lambda_2 > H$	Dark blob

Table 1: Eigenvalues of the local shape descriptor and their associated structure, where H is a suitably high threshold.

Method:

The proposed method follows the HoG based method outlined by Yang, Periaswamy, and Wu [1], but uses a different weighting function for the contribution of each voxel to its respective histogram bin. As is the case in Yang, Periaswamy, and Wu [1], the volume of interest is split into 8 quadrants. Then, within each quadrant, a weighted histogram is generated. The histogram gives a shape descriptor of the quadrant within the volume of interest that is general, sparse and flexible to variations in nodule shape and size.

Within each histogram, 8 bins are used to represent the orientation of the unsigned angle of the 3D gradient projected onto the xy plane, θ_{xy} (allowing for 20 degree increments between bins) and 4 bins are used to represent the orientation of the unsigned angle between the 3D gradient and z axis, θ_z (allowing for 45 degree increments between bins). These angles can be computed as:

$$\theta_{xy}(x,y,z) = \arctan\left(\frac{dy}{dx}\right)$$

$$\theta_z(x,y,z) = \arctan\left(\frac{\sqrt{dx^2 + dy^2}}{dz}\right)$$

In the proposed method, for each voxel in the quadrant that is within the lung volume mask, its contribution the histogram is weighted by its gradient magnitude D_M and by a function of its principal curvature values. The weighting function is chosen based on the outcomes shown in table 1, where the function should respond closer to 1 as the local shape descriptor is more indicative that the structure is a bright blob, respond as 0 for indications of dark structures and closer to 0 for structures whose shape is dominated by a single large principal curvature. Thus, the following function is defined:

$$K(\lambda) = \begin{cases} 1 \ if \ \lambda < -H \\ 0 \ if \ \lambda > 0 \\ 1 - \dfrac{(H - |\lambda|)}{H} \end{cases}$$

Then, the weighting of the voxel for the histogram is computed as:

$$H_i\left(u_{\theta_{xy}}\right) = \sum D_M(x,y,z) \cdot \frac{(1 + K(\lambda_1) + K(\lambda_2) + K(\lambda_3))}{4}$$

Thus, the weighting determined by the principal curvatures is largest for blob structures, and weakens for more cylindrical or plane like shapes. However, it will not completely ignore voxels that do not have the desired shape characteristics. Using this scheme, each volume of interest produces 8 histograms, each consisting of 9 xy orientation bins followed by 4 z orientation bins. Each histogram is normalized by the largest gradient magnitude seen in the respective quadrant and the histograms are scaled based on the size of the volume of interest, to avoid sizing issues between different volumes of interest.

Classification and experimental results:

Once the weighted histograms are generated, they are used as 3D shape descriptors to be classified by a linear SVM. In this case, the linear SVM implementation of dlib [14] is utilized. The training set consists of 100 CT scans taken from the Lung Image Database Consortium (LIDC) [16]. Positive training examples are derived from the labeling included in the data set, whereas 100-200 negative training examples are randomly generated from each CT scan based on volumes consisting of a sufficient number of voxels with large gradient magnitude that occur within the lung volume mask. The results, averaged over 3 fold cross validation of the data set, are compared between the proposed method and a "basic" HoG method. In the basic HoG method, the weighting is determined by the product of the voxel gradient magnitude and a Gaussian Spatial kernel of the distance of the voxel to the volume of interest's center, such that points near the spatial boundary are favored [1].

	Positive samples	Negative samples	Sensitivity	Specificity
Basic HoG	288	537	81.15%	%96.98
Proposed method	288	537	85.37%	%95.45

Table 2: Classifier results for 100 CT scans

The proposed method shows a small increase in sensitivity compared to the traditional HoG model. In particular, it is more robust to volumes of interest that contain a small lesion with weaker gradient magnitudes as well as blood vessels or other anatomical structures (figure 3D). In this case, the proposed method is able to utilize the curvature information to mitigate voxel contributions to histograms that originate from voxels that are a part of irrelevant anatomy. In the case where the nodule is more clearly defined and most of the irrelevant anatomical structure is relatively minor in the volume of interest, both algorithms perform approximately equivalently (figure 2 A, B). However, when curvature information is not entirely reliable because the nodule is very small or attached to the wall of the lung, the proposed method performs worse. In some of these cases the curvature can be misleading, particularly if the nodules is attached to a non-nodule structure that has principal curvature values that would indicate a more blob like structure. This issue occurs more frequently at the edges of the lung volume mask and near to the lung wall, as is the case in figure 2 C. In this situation the proposed method may focus on voxels belonging to the irrelevant anatomical structure as oppose to the nodule, leading to classification issues. Ultimately, while including the curvature information in the voxel weighting shows some benefit in improving detection rate, the increase in false positives is non negligible for automated screening of lung CT scans.

Conclusion and Future work

The proposed method demonstrates that incorporating local curvature information into existing algorithms can provide a benefit for sensitivity. However several improvements could be made to improve the method. The largest improvement could come from using PCA, or a similar method, on the volume of interest to consistently align the voxels according to its principal orientations. In doing so, the method would be more robust to changes in rotation. Additionally the method in which negative training samples are chosen may introduce bias, having a human create a database of negative samples instead of the random sampling approach may improve results and consistency. Finally, the rescaling of histograms based on the size of the volume of interest may also be introducing issues, in general other HoG methods tend to up sample or down sample to a consistent size instead or filter through the image at a series of fixed scales. Finally further investigation could look into whether the proposed method could be extended as a filtering or weighting mechanism for determining the contribution of individual voxels in a volume of interest for other methods as many methods may improve from being able to ignore voxels from irrelevant anatomical structures. The goal of future work should be aimed towards preserving the increase in sensitivity, while reducing the increased rate of false positives.

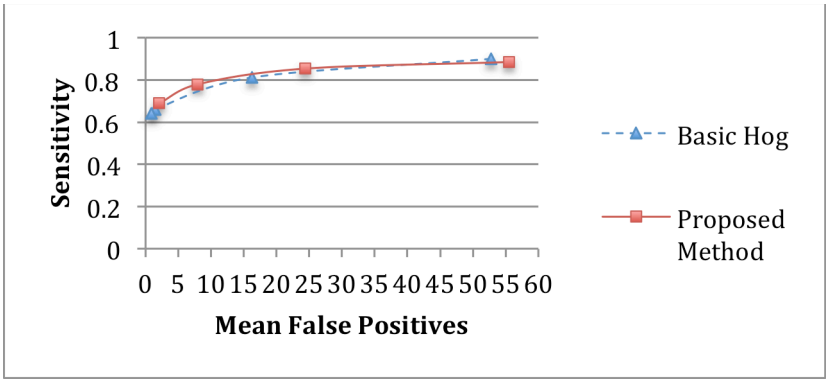

Chart 1: ROC curves of the Basic HoG method and the proposed method.

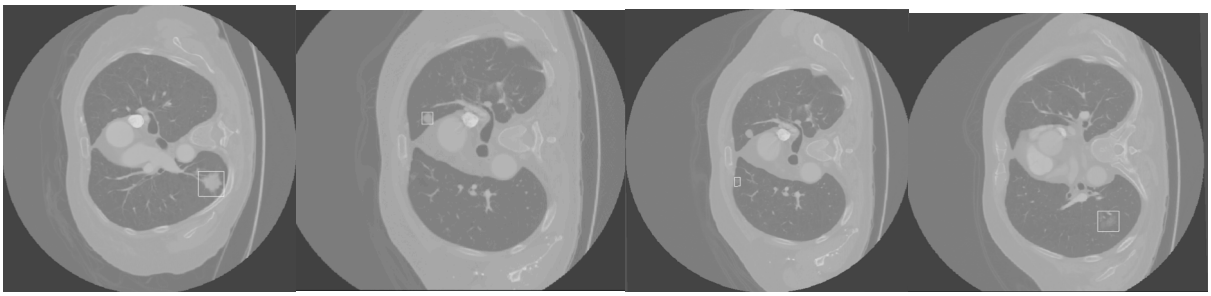

(A) (B) (C) (D)

Figure 3: Samples taken from the dataset, volume of interest indicated by white bounding box

Reference:

1. Yang, Ming, Senthil Periaswamy, and Ying Wu. "False positive reduction in lung GGO nodule detection with 3d volume shape descriptor." *Acoustics, Speech and Signal Processing, 2007. ICASSP 2007. IEEE International Conference on*. Vol. 1. IEEE, 2007.
2. Tan, Maxine, et al. "A novel computer-aided lung nodule detection system for CT images." *Medical physics* 38.10 (2011): 5630-5645.
3. Zhao, Binsheng. Automatic detection of small lung nodules on CT utilizing a local density maximum algorithm. Journal of Applied Clinical Medical Physics, [S.l.], p. 248 - 260, jun. 2003. ISSN 15269914.
4. Ge, Zhanyu, et al. "Computer-aided detection of lung nodules: false positive reduction using a 3D gradient field method and 3D ellipsoid fitting." *Medical physics* 32.8 (2005): 2443-2454.
5. Alilou, Mehdi, et al. "A Comprehensive Framework for Automatic Detection of Pulmonary Nodules in Lung Ct Images." Image Analysis & Stereology 33.1 (2014): 13-27.
6. Sato, Yoshinobu, et al. "Tissue classification based on 3D local intensity structures for volume rendering." *Visualization and Computer Graphics, IEEE Transactions on* 6.2 (2000): 160-180.
7. Mendonça, Paulo RS, et al. "Model-based analysis of local shape for lesion detection in CT scans." *Medical Image Computing and Computer-Assisted Intervention–MICCAI 2005*. Springer Berlin Heidelberg, 2005. 688-695.
8. Sahiner, Berkman, et al. "False-positive reduction using Hessian features in computer-aided detection of pulmonary nodules on thoracic CT images."*Medical Imaging*. International Society for Optics and Photonics, 2005.
9. Epstein, Mark L., Ivan Sheu, and Kenji Suzuki. "Hessian Matrix-Based Shape Extraction and Volume Growing for 3D Polyp Segmentation in CT Colonography."
10. Daniels, Florie, et al. "Quantification of collagen orientation in 3D engineered tissue." *3rd Kuala Lumpur International Conference on Biomedical Engineering 2006*. Springer Berlin Heidelberg, 2007.
11. O'Dell, Walter G. "Automatic segmentation of tumor-laden lung volumes from the LIDC database." SPIE Medical Imaging. International Society for Optics and Photonics, 2012.
12. Monga, Olivier, Rachid Deriche, and Jean-Marie Rocchisani. "3D edge detection using recursive filtering: application to scanner images." *CVGIP: Image Understanding* 53.1 (1991): 76-87.
13. Monga, Olivier, and Serge Benayoun. "Using partial derivatives of 3D images to extract typical surface features." *Computer vision and image understanding*61.2 (1995): 171-189.
14. Davis E. King. Dlib-ml: A Machine Learning Toolkit. Journal of Machine Learning Research 10, pp. 1755-1758, 2009
15. Armato III, Samuel G., et al. "The lung image database consortium (LIDC) and image database resource initiative (IDRI): a completed reference database of lung nodules on CT scans." *Medical physics* 38.2 (2011): 915-931.